

# Approximating Chaotic Saddles for Delay Differential Equations

S. Richard Taylor\*  
Thompson Rivers University

Sue Ann Campbell†  
University of Waterloo  
(Dated: 27 February 2007)

Chaotic saddles are unstable invariant sets in the phase space of dynamical systems that exhibit transient chaos. They play a key role in mediating transport processes involving scattering and chaotic transients. Here we present evidence (long chaotic transients and fractal basins of attraction) of transient chaos in a “logistic” delay differential equation. We adapt an existing method (stagger-and-step) to numerically construct the chaotic saddle for this system. This is the first such analysis of transient chaos in an infinite-dimensional dynamical system, and in delay differential equations in particular. Using Poincaré section techniques, we illustrate approaches to visualizing the saddle set, and confirm that the saddle has the Cantor-like fractal structure consistent with a chaotic saddle generated by horseshoe-type dynamics.

PACS numbers: 05.10.-a, 05.45.Jn, 05.45.Pq, 02.30.Ks

Keywords: chaos, transient chaos, chaotic transient, chaotic saddle, strange repeller, invariant set, delay differential equations

## I. INTRODUCTION

Many physical systems exhibit transient chaos; that is they behave in an erratic, unpredictable way for a period of time, but eventually settle down to rest or to a simple periodic motion. Rolling dice, tossing coins and other means of generating random outcomes are familiar examples. A similar phenomenon is observed in experiments on fluids [1]. Mathematical models also can exhibit long chaotic transients, e.g. the Hénon map [2, 3], coupled Van der Pol oscillators [4] and the kicked double rotor [5]. Despite the diversity of these examples, they are thought to share in common a universal dynamical mechanism, which is the existence in phase space of an unstable, fractal invariant set on which the dynamics are chaotic [2, 6]. This set has been called a *chaotic saddle* (owing to its saddle-type instability) or *strange repeller*.

The existence of a chaotic saddle generates transient chaotic dynamics by the following mechanism. Phase space orbits originating exactly on the saddle remain chaotic for all time, but due to the saddle’s instability these orbits are not experimentally observable. Rather, a typical phase space trajectory enters a neighborhood of the saddle via its stable manifold, and thereafter shadows the saddle for a period of time during which it exhibits the erratic motion associated with the chaotic dynamics on the saddle. After this chaotic transient period the trajectory exits the saddle along its unstable manifold, eventually to be captured by an attracting set (typically a fixed point or periodic orbit, but possibly a chaotic

attractor).

Because the the dynamics on unstable sets cannot be observed directly, it is often asserted that such sets have little relevance to experimental observations. However, in transient chaos it is precisely the transient behavior that is of interest. Indeed, Kantz and Grassberger [2] have argued that, owing to the mechanism described above, a unified understanding of chaotic transients relies on an analysis of the dynamics on the unstable chaotic set.

A fairly complete analysis is possible for systems that exhibit horseshoe-type dynamics [7], such as the celebrated homo- or hetero-clinic chaos that occurs due to the transversal intersection of stable and unstable manifolds of an equilibrium point or periodic orbit [8]. In this situation the saddle is known to be a product of Cantor sets, and the dynamics on it are conjugate to a subshift of finite type (a generalization of the Smale horseshoe [9]), yielding a symbolic coding of the dynamics on the saddle.

However, it is often difficult to obtain rigorous results for realistic models, so that there is an active literature on the numerical detection and approximation of chaotic saddles. Here the essential problem is to construct a numerical trajectory that lies very near the saddle for an arbitrarily long time, the idea being that such a trajectory will shadow a true trajectory on the saddle. This is accomplished by repeatedly making small (i.e. at the limit of numerical precision) perturbations of a numerical trajectory, so that it remains indefinitely within a (small) neighborhood of the saddle. Variations on this theme, differing only in the method of choosing suitable perturbations, include the “straddle-orbit method” [4], “stagger-step method” [5], the “PIM triple procedure” [3], and most recently a gradient search algorithm due to Bollt [10]. All have fairly severe limitations. The straddle-orbit and PIM triple methods apply only if the unstable manifold of the saddle is one-dimensional. The

---

\*Electronic address: rtaylor@tru.ca; URL: <http://cariboo.tru.ca/advtech/math-sta/faculty/rtaylor>

†Electronic address: sacampbell@uwaterloo.ca; URL: <http://www.math.uwaterloo.ca/~sacampbe>

other methods suffer from the exponential growth of phase space volume with dimension, which greatly hinders the search for successful perturbations if the system dimension is greater than about four. The construction of a general-purpose algorithm for approximating chaotic saddles remains an open problem.

In this paper we consider the problem of approximating chaotic saddles for delay differential equations (DDE's). DDE's arise in models of phenomena in which the rate of change of the system state depends explicitly on the state at some past time, as for example in the case of delayed feedback. Neural systems [11], respiration regulation [12], agricultural commodity markets [13], nonlinear optics [14], neutrophil populations in the blood [12, 15], and metal cutting [16] are just a few systems in which delayed feedback leads naturally to models expressed in terms of delay differential equations.

DDE's are also interesting because they serve as prototypical dynamical systems of infinite dimension, for which both numerical and analytical methods are intermediate in complexity between ordinary and partial differential equations. DDE's therefore provide a natural ground for developing numerical methods for the analysis of transient chaos in infinite dimensional systems, much as Farmer [17] has suggested in the context of chaotic attractors.

For simplicity we consider only autonomous, evolutionary delay equations with a single fixed delay time,  $\tau$ , modeling a process  $x(t) \in \mathbb{R}$  satisfying

$$\frac{dx(t)}{dt} = f(x(t), x(t - \tau)) \quad (1)$$

for some  $f : \mathbb{R}^2 \rightarrow \mathbb{R}$ . Most of the ideas presented here have obvious generalizations to more general autonomous DDE's, e.g. with higher dimension, multiple delays, time varying or distributed delays, and higher derivatives.

Aside from unpublished work referenced in [2], to date there has been no account of transient chaos in delay differential equations. However, there is substantial evidence that transient chaos occurs in some DDE's. The present study was motivated by the observations in [18, 19] of fractal basins of attraction (a hallmark of transient chaos [6]) in delay equations<sup>1</sup>. Transverse homoclinic orbits (hence horseshoe dynamics) have also been proved to occur in some DDE's [20–22], and there is numerical evidence [23] for transverse homoclinic orbits in the Mackey-Glass equation [15]. These results have been presented in discussions of attracting chaos, whereas transient chaos in DDE's has not been specifically investigated. In particular, no attempt has been made to identify and construct a chaotic saddle.

In the present work we investigate fractal basins of attraction and transient chaos for DDE's, taking a particular “logistic” DDE as an example. We develop an implementation of the stagger-step method applicable to DDE's of the form (1), and use it to construct and visualize the chaotic saddle for our example.

Since the saddle is embedded in an infinite dimensional phase space, it is difficult to visualize. We explore various approaches to visualizing the saddle by using projections onto  $\mathbb{R}^2$  and  $\mathbb{R}^3$ , and Poincaré section techniques to achieve further reductions in dimension. While being the first such investigation for DDE's in particular, the present work is also novel for giving the first numerical construction of a chaotic saddle for a dynamical system of infinite dimension. This work paves the way for a similar approach to other infinite-dimensional systems, for instance systems modeled by evolutionary PDE's.

## II. BACKGROUND ON DELAY DIFFERENTIAL EQUATIONS

We consider one-dimensional autonomous delay differential equations of the form (1) with  $x(t) \in \mathbb{R}$ ,  $t \geq 0$ . Properties of such DDE's and their solutions can be found e.g. in [24, 25]. Here we summarize the most essential facts relevant to our work.

Without loss of generality we can take the delay time  $\tau$  to be 1, achieved by an appropriate re-scaling of the time  $t$  in equation (1). Thus the DDE's we consider have the form

$$x'(t) = f(x(t), x(t - 1)). \quad (2)$$

For equation (2) to define a unique solution  $x(t)$ , say for all  $t \geq 0$ , initial data must be furnished in the form of values  $x(t)$  for all  $-1 \leq t \leq 0$ . Otherwise, the right-hand side will fail to be defined for some  $t \in [0, 1]$ . In order that equation (2) prescribes a well-defined evolutionary process, we assume that  $f$  is such<sup>2</sup> that for any continuous “initial function”  $\phi : [-1, 0] \rightarrow \mathbb{R}$ , there is a unique solution  $x(t)$  satisfying (2) for all  $t > 0$ , and the initial condition

$$x(t) = \phi(t), \quad t \in [-1, 0]. \quad (3)$$

The DDE (2) can be regarded as a dynamical system on the infinite-dimensional phase space  $C \equiv C[-1, 0]$ , the space of continuous functions on the interval  $[-1, 0]$ . To see how this can be so (see for example [25, 26]), consider that a solution  $x(t)$  is uniquely determined for all  $t > 0$  only if initial data are given for all  $t \in [-1, 0]$ , in the manner of equation (3). More generally the continuation

<sup>1</sup> In the DDE studied in [18] fractal basins are present even in the absence of a delay. Our focus here is on systems where the dynamical instability is caused by the delay.

<sup>2</sup> e.g.  $f \in C^1$  and  $|f(u, v)| \leq N(t) \max\{|u|, |v|\}$  for some positive continuous function  $N(t)$  [24].

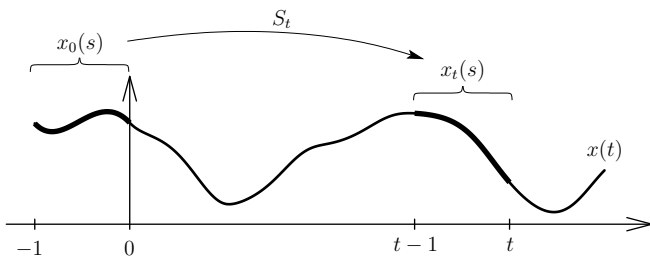


FIG. 1: Action of the evolution operator  $S_t$  for a DDE. A given initial function  $\phi = x_0 \in C$  generates a solution  $x(t)$  of the initial value problem (2)–(3), which in turn defines the phase point  $x_t \in C$  at time  $t$ .  $S_t$  is the operator on  $C$  that takes  $x_0$  to  $x_t$ .

of a solution for  $t > T$  is uniquely determined by its history on the interval  $[T - 1, T]$ . Let the function

$$x_t(s) = x(t + s), \quad s \in [-1, 0] \quad (4)$$

represent the segment of a given solution  $x(t)$  on the *delay interval*  $[t - 1, t]$ . Since  $x_t$  uniquely determines  $x_{t'}$  for any  $0 \leq t \leq t'$ , we can take  $x_t$  to be the phase point, at time  $t$ , for the corresponding dynamical system. By virtue of continuity of solutions of (2),  $x_t \in C$  for all  $t \geq 0$  so we take the phase space to be  $C$ .

For each  $t \geq 0$  let  $S_t : C \rightarrow C$  be the evolution operator that takes  $x_0$  to  $x_t$ . That is,

$$S_t(x_0) = x_t \quad (5)$$

where  $x_t(s) \equiv x(t + s)$  and  $x(t)$  is the solution of (2)–(3) corresponding to the initial function  $\phi = x_0 \in C$ . Since the DDE is autonomous, it is invariant under time translation, so that  $S_t$  has the semigroup property [25]:  $S_0$  is the identity transformation, and  $S_{t+t'} = S_t \circ S_{t'}$  for all  $t, t' \geq 0$ . Thus the family of transformations  $\{S_t : t \geq 0\}$  determine a continuous-time dynamical system on  $C$ .

Figure 1 illustrates the relationship of the evolution operator  $S_t$  to a given solution  $x(t)$  of the DDE. The action of  $S_t$  on a function  $x_0 \in C$  has a simple geometric interpretation: it consists of continuing the initial function  $\phi = x_0$  as a solution  $x(t)$  of the DDE, restricting the resulting function to the interval  $[t - 1, t]$ , then translating this function to time 0.

For a given initial function  $\phi \in C$ , we can recast the DDE problem (2)–(3) as an abstract initial value problem in  $C$ , as follows,

$$\begin{cases} x_t = S_t(x_0), & t \geq 0 \\ x_0 = \phi. \end{cases} \quad (6)$$

This initial value problem determines a trajectory  $\{x_t : t \geq 0\} \subset C$ . Any given solution of (2) is thereby identified with a particular trajectory in  $C$ . For example, a periodic solution of the DDE corresponds to a periodic orbit, i.e. a trajectory that lies on an invariant closed curve in  $C$ . This identification of DDE solutions with

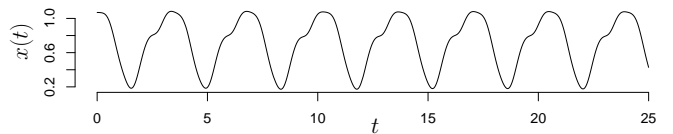


FIG. 2: The asymptotically stable periodic solution for the logistic DDE (7) with  $\lambda = 6.16$ . The period is approximately 3.38.

phase space objects allows one to study the DDE dynamics using the tools and concepts of dynamical systems theory.

### III. BASINS OF ATTRACTION

For illustrative purposes we consider the “logistic” delay differential equation

$$x'(t) = -x(t) + \lambda x(t - 1)[1 - x(t - 1)] \quad (7)$$

where  $\lambda$  is a real parameter. For  $\lambda$  near 6.16 we find that there is just one asymptotically stable periodic solution, whose graph is shown in Fig. 2. In numerical experiments, every solution of (7) exhibits one of two possible asymptotic behaviors: it is either eventually asymptotic to the periodic solution, or else eventually diverges to  $-\infty$ . These two asymptotic behaviors correspond to two attractors in the phase space  $C$  for the dynamical system  $S_t$  — one an attracting periodic orbit  $\Gamma$ , the other an attractor “at infinity”. The set of initial functions  $\phi \in C$  such that  $S_t(\phi) \rightarrow \Gamma$  constitutes the periodic solution’s *basin of attraction*,  $\beta(\Gamma)$ .

Suppose  $x(t)$  is an asymptotically stable periodic solution for the DDE (2). Let  $\Gamma \subset C$  be the corresponding periodic orbit for the dynamical system  $S_t$ . The basin of attraction for  $\Gamma$  is the set of initial functions  $\phi \in C$  such that the orbit  $\{S_t(\phi) : t \geq 0\}$  converges to  $\Gamma$ , i.e.,

$$\beta(\Gamma) \equiv \{\phi \in C : S_t(\phi) \rightarrow \Gamma \text{ as } t \rightarrow \infty\}. \quad (8)$$

Since the basin of attraction is a subset of the infinite-dimensional space  $C$ , it is difficult to visualize. By graphing its intersection with some two-dimensional subset of  $C$  we can gain some insight into the geometry of this set (a similar technique is used in [19]).

Figure 3 shows a sequence of images, at increasing levels of magnification, of the basins of attraction for the logistic DDE (7). For each point  $(A, B)$  on a  $2048 \times 2048$  uniform grid, we compute a numerical solution generated by the initial function

$$\phi(t) = A + \sin(B(t + 1)), \quad t \in [-1, 0]. \quad (9)$$

If this solution is eventually asymptotic to the periodic solution shown in Fig. 2, then the function  $\phi$  lies in the basin of attraction  $\beta(\Gamma)$ , and we plot a pixel at the corresponding point  $(A, B)$ . Otherwise, the solution diverges to  $-\infty$ , and  $\phi$  does not lie in  $\beta(\Gamma)$ . In this way we obtain

an image in which the set of black pixels approximate the basin of attraction for the periodic solution  $\Gamma$ . More precisely, the image represents part of the intersection of  $\beta(\Gamma)$  with the 2-dimensional subset<sup>3</sup> of  $C$  consisting of functions  $\phi$  of the form (9), parametrized by  $(A, B) \in \mathbb{R}^2$ .

The basins of attraction shown in Fig. 3 have a self-similar fractal structure; their boundaries appear to be the product of a curve and a Cantor set. This structure is typical of basins of attraction for dynamical systems that exhibit transient chaos and possess an invariant unstable set on which the dynamics are chaotic [4, 7, 27]. Phase points on the basin boundaries lie on unstable invariant sets in  $C$ , such as unstable periodic orbits, chaotic saddles, and their stable manifolds. The fractal structure of the boundaries therefore reflects the fractal structure of a supposed chaotic saddle. We conjecture that the dynamical system  $S_t$  does possess such a chaotic saddle, and in the following sections we seek to construct and visualize the saddle and analyze the dynamics on it.

From the intricate structure of the basins shown in Fig. 3 it is apparent that the DDE (7) must exhibit a form of sensitivity to initial conditions (final state dependence [27]), at least for initial functions near the basin boundary. Initial phase points near the boundary are expected to shadow the saddle's stable manifold, and to exhibit the associated chaotic dynamics for some time before converging to one or the other of the two attractors.

Indeed, solutions of equation (7) with long chaotic transients are readily found. Figure 4 shows numerical solutions corresponding to two near-identical initial functions,  $\phi_1$  and  $\phi_2$ , differing by one part per million. Both exhibit a transient chaotic period in which the solution behaves erratically, followed eventually by convergence to the attracting periodic solution. The solutions diverge rapidly for  $t > 30$  and remain uncorrelated during the chaotic phase of their evolution. However, this sensitivity to initial conditions occurs only during the transient phase, as both solutions eventually exhibit the same asymptotic behavior of convergence to the attracting periodic orbit.

## IV. APPROXIMATING THE SADDLE

### A. Discretizing the Delay Equation

Analytical tools for studying DDE's are few, and in practice one must usually resort to numerical simulations. Thus, while it is useful to view a DDE as a dynamical system  $S_t$  on the infinite-dimensional phase space  $C$ , by discretizing the delay equation one effectively in-

troduces a finite-dimensional dynamical system that approximates  $S_t$ . It is to this approximate system that we apply the stagger-step method, in order to approximate chaotic saddles for DDE's.

Any fixed time-step integration method furnishes approximate solution values  $x_n \equiv x(nh)$  at times  $t = nh$  ( $n = 0, 1, 2, \dots$ ) on a uniform grid, where  $h$  is the time step. We choose  $h = 1/M$  so that the delay interval  $[-1, 0]$  is discretized into an integer number  $M$  of equal subintervals. For ease of notation fix  $N = M + 1$ . Then at time step  $n$  the vector

$$\mathbf{u}^n = (x_{n-M}, \dots, x_{n-1}, x_n) \in \mathbb{R}^N \quad (10)$$

provides a discretized representation of the phase point function  $x_t(s) \in C$ . In the literature on numerical solution of DDE's,  $\mathbf{u}^n$  is the "history queue" at time step  $n$ .

The basic integration time step that takes  $\mathbf{u}^n$  to  $\mathbf{u}^{n+1}$  implicitly defines a map  $G : \mathbb{R}^N \rightarrow \mathbb{R}^N$ , such that  $\mathbf{u}^{n+1} = G(\mathbf{u}^n)$ . (By contrast, recall that for a scalar ordinary differential equation one time step is effected by an analogous transformation  $G : \mathbb{R} \rightarrow \mathbb{R}$ .) This map approximates the action of the time- $h$  evolution operator  $S_h$  (c.f. equation (5)). Thus we regard  $G$  as a discrete-time dynamical system on  $\mathbb{R}^N$ , that approximates the corresponding discrete-time system  $S_h$  on  $C$ .

A single integration time step makes only an incremental change to  $\mathbf{u}^n$  on the order of the time step  $h$ , so that it is convenient to define  $F = G^N$  to be the dynamical system on  $\mathbb{R}^N$  that carries out  $N$  integration time steps. Thus  $F$  approximates the action of the time-one solution map  $S_1$  taking the function  $x_t(s)$  to  $x_{t+1}(s)$ .

In our implementation we use a fifth-order Runge-Kutta time step to integrate from  $x_n$  to  $x_{n+1}$ , with  $N = 250$  and therefore a time step  $h = 0.004$ . Piecewise cubic polynomial interpolation is used for evaluation of  $x(t - 1)$  at times that do not coincide with the uniform grid.

### B. Applying the Stagger-Step Method

We use the stagger-step method [5] to find arbitrarily long chaotic solutions  $x(t)$  and thereby construct the supposed chaotic saddle, for the numerical dynamical system  $F$  on  $\mathbb{R}^N$  that approximates the time-one solution map for the logistic DDE (7). The details of the implementation are as follows. Throughout, we take the norm on  $\mathbb{R}^N$  to be the max-norm  $\|\mathbf{u}\| = \max_i |u_i|$ , both for the sake of computational efficiency and because it gives a natural approximation of the sup-norm on the function space  $C$ .

The stagger-step method requires that one define a suitable *restraining region*  $R \subset \mathbb{R}^N$  that contains no attractor for  $F$ . To this end we take  $R$  to be the ball  $\{\mathbf{u} \in \mathbb{R}^N : \|\mathbf{u}\| < 30\}$ , from which are deleted all points

<sup>3</sup> The chosen form for the initial functions  $\phi$  given by equation (9) is somewhat arbitrary. Any two-parameter family of functions in  $C$  would do, provided this set intersects  $\beta(\Gamma)$ .

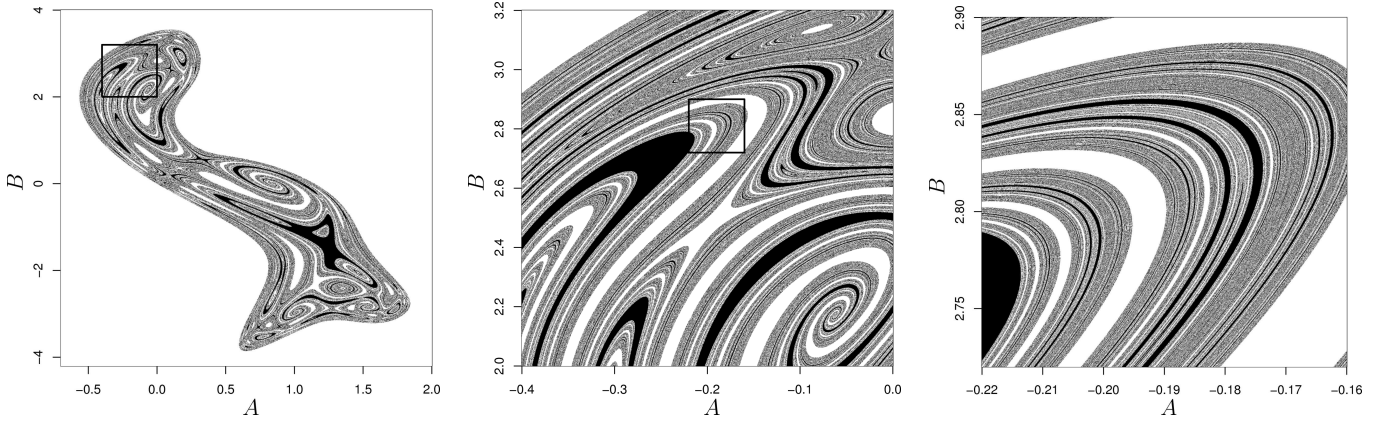


FIG. 3: Basins of attraction for the logistic DDE (7). From left to right, each image shows an enlargement of the boxed region in the previous image. For initial functions of the form  $\phi(t) = A + \sin(Bt)$ ,  $t \in [0, 1]$ , a pixel is plotted at the point  $(A, B)$  if the corresponding solution is asymptotic to the periodic solution shown in Fig. 2. White pixels correspond to initial functions that generate solutions diverging to  $-\infty$ .

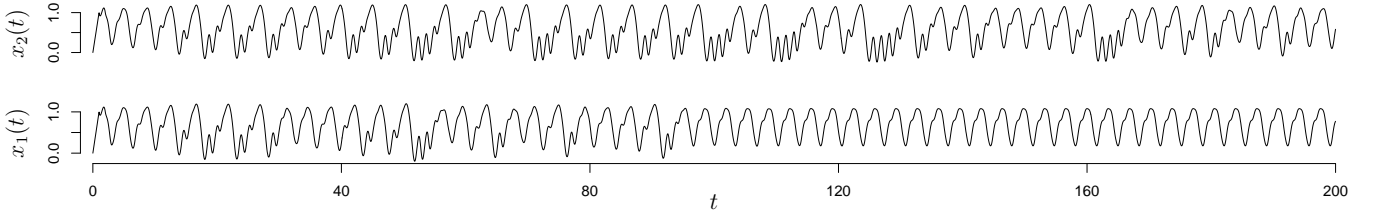


FIG. 4: Numerical solutions of the logistic DDE (7), illustrating chaotic transients and sensitive dependence on initial conditions. The solutions correspond to near-identical initial functions  $\phi_1(t) = t$  ( $t \in [0, 1]$ ) and  $\phi_2 = \phi_1 + 10^{-6}$ .

within a distance  $\varepsilon = 10^{-2}$  of the attracting periodic<sup>4</sup> orbit  $\Gamma$  that corresponds to the asymptotically stable periodic solution shown in Fig. 2. Thus  $R$  excludes both the attractor  $\Gamma$  and the attractor at infinity.

For each  $\mathbf{u} \in R$  define the *transient lifetime*

$$T(\mathbf{u}) = \min\{n \geq 0 : F^n(\mathbf{u}) \notin R\}. \quad (11)$$

We set  $T(\mathbf{u}) = \infty$  if  $F^n(\mathbf{u}) \in R$  for all  $n \geq 0$ ; thus the set of phase points  $\mathbf{u}$  such that  $T(\mathbf{u}) = \infty$  constitute an invariant set that contains the chaotic saddle. The stagger-step method is motivated by the intuitive idea (justified in [3]) that where  $T(\mathbf{u})$  is large,  $\mathbf{u}$  should be close to the saddle. For  $R$  as defined in the preceding paragraph, we calculate  $T(\mathbf{u})$  as the number of iterations of  $F$  required to take  $\mathbf{u}^n = F^n(\mathbf{u})$  either outside a ball of radius 30 or to within  $\varepsilon$  of the attracting periodic solution.

For a given  $0 < \delta \ll 1$  and  $T_* \gg 1$  (we take  $\delta = 10^{-10}$  and  $T_* = 90$ ) the goal of the stagger-step method is to find a  $\delta$ -pseudo-trajectory for  $F$ ; that is, a trajectory  $\{\mathbf{u}^n : n \geq 0\}$  such that

$$\|F(\mathbf{u}^n) - \mathbf{u}^{n+1}\| < \delta$$

and  $T(\mathbf{u}^n) \geq T_*$  for all  $n$ . This is accomplished by iterating as follows:

$$\mathbf{u}^{n+1} = \begin{cases} F(\mathbf{u}^n) & \text{if } T(\mathbf{u}^n) > T_* \\ F(\mathbf{u}^n + \mathbf{r}^n) & \text{otherwise,} \end{cases} \quad (12)$$

where  $\mathbf{r}^n \in \mathbb{R}^N$  is a randomly chosen *stagger*, with  $\|\mathbf{r}^n\| < \delta$ , such that  $T(\mathbf{u}^n + \mathbf{r}^n) > T_*$ . The direction of  $\mathbf{r}^n$  is chosen randomly with uniform distribution on an  $N$ -sphere. Following the suggestion of [5], the search for a successful stagger is made more efficient by randomly choosing the magnitude  $\|\mathbf{r}^n\|$  from an exponential distribution, such that  $\log_{10} \|\mathbf{r}^n\|$  is distributed uniformly on the interval  $(-15, -10)$ . Stagers  $\mathbf{r}^n$  are sampled from this distribution until one is found satisfying  $T(\mathbf{u}^n + \mathbf{r}^n) > T_*$ .

Using this algorithm we are able to find stagger-step trajectories  $\{\mathbf{u}^n \in \mathbb{R}^N : n > 0\}$  that lie entirely within the restraining region  $R$  for arbitrarily long times. We find that every such trajectory appears to be aperiodic, and we suppose therefore that  $\mathbf{u}^n$  is eventually very near the chaotic saddle after some transient number of iterations during which  $\mathbf{u}^n$  approaches the saddle along its stable manifold. Furthermore, different runs of the stagger-step algorithm, with different starting conditions and different sequences of random stagers, all generate saddle trajectories that appear to have the same geom-

<sup>4</sup> The attracting set for the discrete-time system  $F \approx S_h$  will be *quasi*-periodic if the solution's period is an irrational multiple of the time step  $h$ .

etry and statistics as reported in the following section, suggesting that there is a unique chaotic saddle on which the dynamics are ergodic.

By the relationship (10), corresponding to any stagger-step trajectory is a time series  $\{x_n\}$  which agrees, within precision  $\delta$ , with a numerical solution of the DDE. By construction this solution exhibits an arbitrarily long chaotic transient. Indeed, time series constructed in this way are qualitatively very similar to those shown in Fig. 4, except that convergence to the periodic solution or to the attractor at infinity is deferred indefinitely.

## V. VISUALIZING THE SADDLE

Phase space objects for delay equations, being subsets of the infinite-dimensional phase space  $C$ , pose significant challenges for visualization. Despite our discretization, which approximates the DDE by a finite-dimensional dynamical system on  $\mathbb{R}^N$ , this difficulty remains because of the large dimension  $N$  (250 in our implementation).

One technique that has been used for visualizing phase-space objects for DDE's is to plot in two dimensions the curve described by the point  $(x(t), x(t-1))$  for a given solution  $x(t)$ . This construction can be interpreted as a projection, from  $C$  into  $\mathbb{R}^2$ , of the corresponding phase space orbit  $\{x_t\} \subset C$ , according to the mapping

$$x_t \in C \mapsto (x_t(0), x_t(-1)) \in \mathbb{R}^2. \quad (13)$$

Figure 5 shows such a projection of a stagger-step trajectory constructed, as described in the preceding section, for the logistic DDE (7). This trajectory appears to be aperiodic, consistent with our supposition that the stagger-step trajectory approximates a true trajectory on a chaotic invariant set.

Sensitive dependence on initial conditions, e.g. as illustrated in Fig. 4, provides further evidence for chaotic dynamics of saddle trajectories. The Lyapunov spectrum on a saddle trajectory provides a quantitative indicator of the degree of sensitive dependence near the saddle. Using standard techniques [17, 28, 29] applied to orbits of the time-one map  $F$  near the saddle, we estimate the five greatest base-2 Lyapunov exponents to be 0.53, 0.00,  $-1.06$ ,  $-1.56$  and  $-2.01$  (independent runs of the stagger-step algorithm, differing in their initial conditions and the sequence of random staggers, reproduce these exponents to the number of decimal places given). That is, two near-identical phase points originating near the saddle will typically diverge exponentially as  $2^{0.53n}$  during their transient period. In information-theoretic terms [30], the chaotic transients generated by the DDE (7) produce on average 0.53 bits of information per unit time. In geometrical terms, we see that the saddle has just one unstable direction along which trajectories diverge exponentially. (The zero exponent corresponds to the direction tangent to the flow  $S_t$ .) Note, however, that the positive Lyapunov exponent is based on a trajectory *on the unstable saddle set*, and signifies

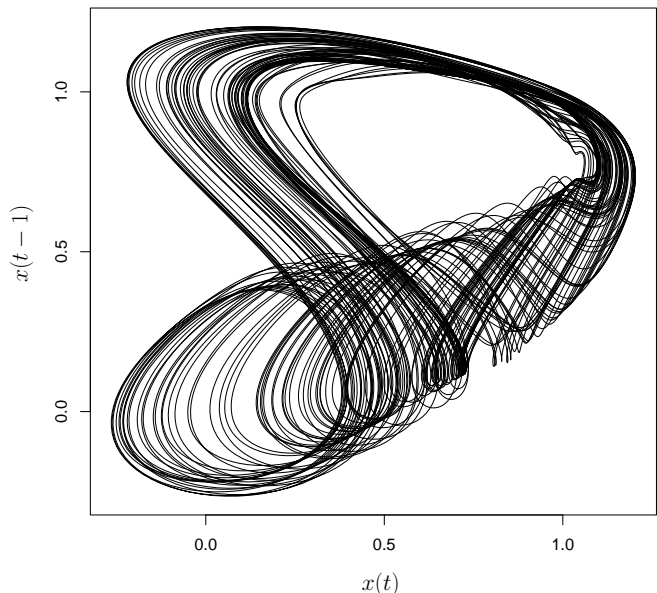


FIG. 5: Projection of a trajectory on the chaotic saddle onto  $\mathbb{R}^2$ , for the logistic DDE (7). We plot the trajectory of the point  $(x(t), x(t-1))$ , where  $x(t)$  is a chaotic solution constructed using the stagger-step algorithm.

exponential divergence only for phase space trajectories near the saddle. After a transient period, initially divergent trajectories may in fact converge on the same attracting period orbit.

The correlation dimension [31] is frequently used as a quantitative indicator of the geometry of complex phase space objects. Using standard time-delay embedding techniques [32] applied to a long chaotic time series  $\{x_n\}$  constructed from a saddle trajectory, we estimate the correlation dimension of the chaotic saddle to be  $2.2 \pm 0.1$ . Thus the saddle appears to be a fractal invariant set, of dimension intermediate between 2 and 3, on which the dynamics are chaotic.

As the saddle's dimension is greater than 2 it is not surprising that its projection shown in Fig. 5 fails to be one-to-one. However, we can hope to obtain a more faithful representation by projecting the saddle into  $\mathbb{R}^3$ , and using Poincaré section methods to obtain a further reduction in dimension. Figure 6 shows a saddle trajectory plotted in  $\mathbb{R}^3$  under the projection

$$\begin{aligned} x_t \in C \mapsto (x_t(0), x_t(-0.5), x_t(-1)) \in \mathbb{R}^3 \\ = (x(t), x(t-0.5), x(t-1)). \end{aligned} \quad (14)$$

Also shown are a series of cross-sections (slices perpendicular to the  $x(t)$ -axis) through the resulting 3-dimensional set, which show more clearly the geometric structure of the saddle. At each cross-section we plot the points of intersection of the saddle trajectory with a plane  $x(t) = x^*$ . This procedure constructs a Poincaré section through the saddle set, with “surface of section”

$$\Sigma = \{x_t \in C : x_t(0) = x^*\}, \quad (15)$$

which is then projected onto  $\mathbb{R}^3$  under the map prescribed by equation (14).

The Poincaré section with surface of section  $x^* = 1$  is shown in detail, at two levels of magnification, in Fig. 7. In these images it appears that the projection in equation (14) is one-to-one almost everywhere on the saddle. That is, with the exclusion of points where the projection fails to be one-to-one, the projection results in a faithful reconstruction or embedding [32] of the saddle in  $\mathbb{R}^3$ . Figure 7 is qualitatively very similar to chaotic saddles for the systems investigated in [2–4, 10], and suggests that the saddle has the fractal structure of a product of Cantor sets, as would be the case with horseshoe-type dynamics [4, 7].

## VI. CONCLUSIONS

Here, for the first time, we have investigated transient chaos in delay differential equations, and we have given the first numerical construction of a chaotic invariant set for the corresponding infinite-dimensional dynamical system. Using the logistic DDE (7) as an example, we have shown the existence of fractal basins of attraction and solutions exhibiting long chaotic transients. These phenomena suggest the existence of a chaotic invariant set in the infinite-dimensional phase space  $C[-1, 0]$ .

Using the stagger-step method we are able to construct arbitrarily long aperiodic trajectories that appear to lie on an unstable invariant set of fractal dimension (i.e. a chaotic saddle or strange repeller). Although the saddle itself arises in an infinite-dimensional phase space, it appears to be a set of relatively low dimension, having e.g. a correlation dimension of about 2.2. By a combination of projection and Poincaré section techniques we are able to visualize a two-dimensional cross-section through this set, and thereby confirm that the saddle has a Cantor-like fractal structure that is consistent with the presence of horseshoe-type dynamics.

There are a number of competing approaches to the approximation of chaotic saddles. The stagger-step method appeared *a priori* to be the best choice here, because of the high-dimensionality of our problem and because other methods are applicable only if the saddle has just one unstable dimension. However, for the logistic DDE we have used for illustration, the saddle turns out to have just one unstable dimension. Therefore other techniques for approximating the saddle should be effective, and as these are expected to be more efficient this is a promising direction for further investigation.

The work presented here is also novel in that it gives the first application of numerical methods for the construction of a chaotic saddle to an *infinite*-dimensional dynamical system. Previous authors have cited the “curse of dimensionality” as a challenge inherent in approximating saddles systems in more than a few dimensions. To our knowledge the investigation in [10] of a 9-dimensional system of ordinary differential equations has until now been the the most ambitious in this regard. Our successful construction of a chaotic saddle in infinite dimensions represents a major step forward. In particular, the ideas presented here should be generalizable in a straightforward way not only to more general DDE’s, but also to evolutionary partial differential equations modeling physical systems of interest, for example in turbulence of fluids. Extending our numerical approach to evolutionary PDE’s is an obvious and potentially rich area for further investigation.

## Acknowledgments

This research was supported by the Natural Sciences and Engineering Research Council through the Post-Graduate Scholarship Program (SRT) and the Discovery Grants Program (SAC). We used the R language [33] for all software implementations.

- 
- [1] A. G. Darbyshire and T. Mullin, *J. Fluid Mech.* **289**, 83 (1995).
  - [2] H. Kantz and P. Grassberger, *Physica D* **17**, 75 (1985).
  - [3] H. E. Nusse and J. A. Yorke, *Physica D* **36**, 137 (1989).
  - [4] P. M. Battelino, C. Grebogi, E. Ott, J. A. Yorke, and E. D. Yorke, *Physica D* **32**, 296 (1988).
  - [5] D. Sweet, H. E. Nusse, and J. A. Yorke, *Phys. Rev. Lett.* **86**, 2261 (2001).
  - [6] T. Tél, in *Experimental study and characterization of chaos*, edited by H. Bai-Lin (World Scientific, Singapore—New Jersey—London—Hong Kong, 1990), vol. 3 of *Directions in Chaos*, pp. 149–211.
  - [7] J. Guckenheimer and P. Holmes, *Nonlinear oscillations, dynamical systems, and bifurcations of vector fields*, vol. 42 of *Applied Mathematical Sciences* (Springer-Verlag, 1983).
  - [8] S. Wiggins, *Global Bifurcations and Chaos* (Springer-Verlag, New York, 1988).
  - [9] S. Smale, *Bull. Amer. Math. Soc.* **73**, 747 (1967).
  - [10] E. M. Bollt, *Int. J. Bifurcation and Chaos* **15**, 1615 (2005).
  - [11] U. an der Heiden, *J. Math. Biol.* **8**, 345 (1979).
  - [12] L. Glass and M. C. Mackey, *Annals of the New York Academy of Science* **316**, 214 (1979).
  - [13] M. C. Mackey, *J. Econ. Theory* **48**, 497 (1989).
  - [14] H. M. Gibbs, *Optical bistability: Controlling light with light* (Academic, Orlando, 1985).
  - [15] M. C. Mackey and L. Glass, *Science* **197**, 287 (1977).
  - [16] G. Stépán, in *Dynamics and Chaos in Manufacturing Processes*, edited by F. Moon (Wiley, New York, 1998), pp. 165–191.
  - [17] J. D. Farmer, *Physica D* **4**, 366 (1982).
  - [18] J. M. Aguirregabiria and J. R. Etxebarria, *Phys. Lett. A* **122**, 241 (1987).

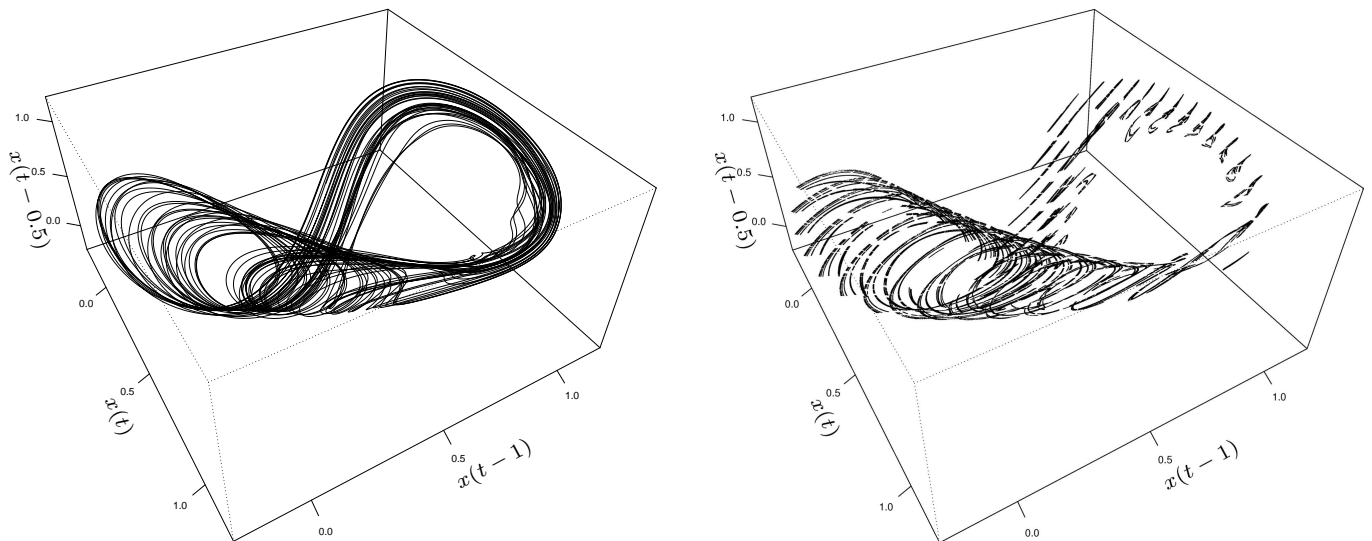


FIG. 6: Projection of the chaotic saddle onto  $\mathbb{R}^3$ , for the logistic DDE (7). The first image shows a single trajectory on the saddle: we plot the trajectory of the point  $(x(t-1), x(t-0.5), x(t))$ , where  $x(t)$  is a chaotic solution constructed using the stagger-step algorithm. The second image shows a series of Poincaré sections through this trajectory.

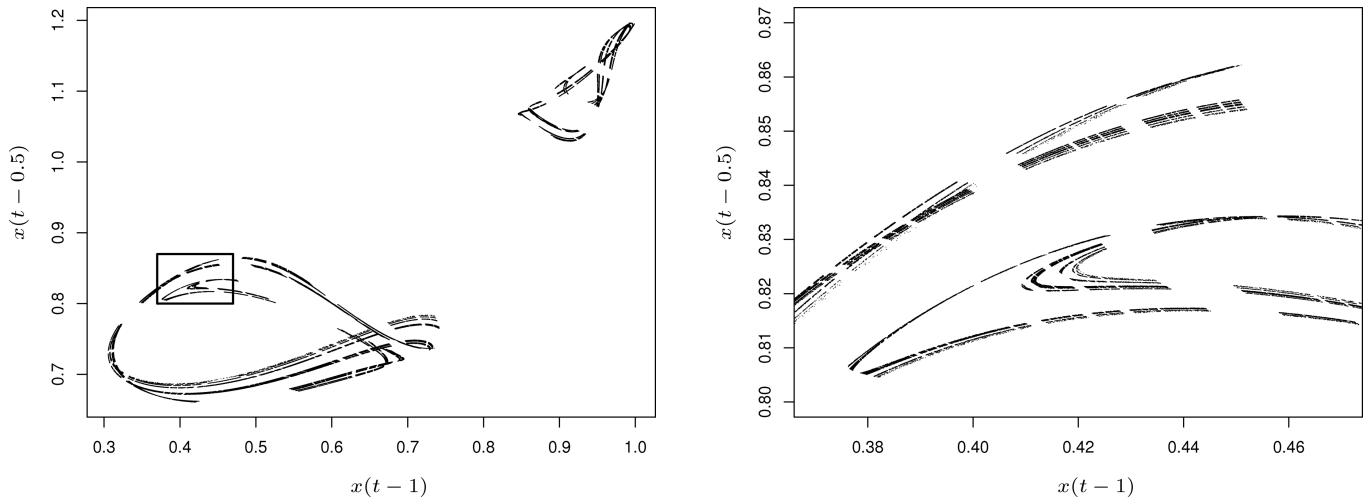


FIG. 7: Poincaré section through the chaotic saddle for the logistic DDE (7), with “surface of section”  $x(t) = 1$ . For a chaotic solution  $x(t)$  constructed using the stagger-step algorithm, a pixel is plotted at the point  $(x(t-1), x(t-0.5))$  whenever  $x(t) = 1$ .

- [19] J. Losson, M. C. Mackey, and A. Longtin, *Chaos* **3**, 167 (1993).
- [20] U. an der Heiden and M. C. Mackey, *J. Math. Biol.* **16**, 75 (1982).
- [21] U. an der Heiden and H.-O. Walther, *J. Diff. Eq.* **47**, 273 (1983).
- [22] H.-O. Walther, *Nonlinear Analysis* **5**, 775 (1981).
- [23] J. K. Hale and N. Sternberg, *J. Comp. Phys.* **77**, 221 (1988).
- [24] R. D. Driver, *Ordinary and delay differential equations* (Springer-Verlag, New York, 1977).
- [25] J. K. Hale and S. M. V. Lunel, *Introduction to functional differential equations*, vol. 99 of *Applied Mathematical Sciences* (Springer-Verlag, New York, 1993).
- [26] O. Diekmann, S. A. van Gils, S. M. V. Lunel, and H.-O. Walther, *Delay equations: Functional, complex and nonlinear analysis*, vol. 110 of *Applied Mathematical Sciences* (Springer-Verlag, New York, 1995).
- [27] S. W. McDonald, C. Grebogi, E. Ott, and J. A. Yorke, *Physica D* **17**, 125 (1985).
- [28] G. Benettin, L. Galgani, A. Giorgilli, and J.-M. Strelcyn, *Meccanica* **15**, 9 (1980).
- [29] G. Benettin, L. Galgani, A. Giorgilli, and J.-M. Strelcyn, *Meccanica* **15**, 21 (1980).
- [30] R. Shaw, *Zeitschrift fur Naturforschung* **36a**, 80 (1981).
- [31] P. Grassberger and I. Procaccia, *Phys. Rev. Lett.* **50**, 346 (1983).
- [32] T. Sauer, J. A. Yorke, and M. Casdagli, *J. Stat. Phys.* **65**, 579 (1991).
- [33] R Development Core Team, *R: A Language and Environment for Statistical Computing*, R Foundation for Statistical Computing, Vienna, Austria (2006).